ARTICLE OPEN

Check for updates

Remote photobiomodulation ameliorates behavioral and neuropathological outcomes in a rat model of repeated closed head injury

Chongyun Wu[1], Meng Li[1], Zhe Chen[1], Shu Feng[1], Qianting Deng[1], Rui Duan[2], Timon Cheng-Yi Liu[3] and Luodan Yang[1]✉

Repeated closed-head injuries (rCHI) from activities like contact sports, falls, military combat, and traffic accidents pose a serious risk due to their cumulative impact on the brain. Often, rCHI is not diagnosed until symptoms of irreversible brain damage appear, highlighting the need for preventive measures. This study assessed the prophylactic efficacy of remote photobiomodulation (PBM) targeted at the lungs against rCHI-induced brain injury and associated behavioral deficits. Utilizing the "Marmarou" weight-drop model, rCHI was induced in rats on days 0, 5, and 10. Remote PBM, employing an 808 nm continuous wave laser, was administered daily in 2-min sessions per lung side over 20 days. Behavioral deficits were assessed through three-chamber social interaction, forced swim, grip strength, open field, elevated plus maze, and Barnes maze tests. Immunofluorescence staining and 3D reconstruction evaluated neuronal damage, apoptosis, degeneration, and the morphology of microglia and astrocytes, as well as astrocyte and microglia-mediated excessive synapse elimination. Additionally, 16S rDNA amplicon sequencing analyzed changes in the lung microbiome following remote PBM treatment. Results demonstrated that remote PBM significantly improved depressive-like behaviors, motor dysfunction, and social interaction impairment while enhancing grip strength and reducing neuronal damage, apoptosis, and degeneration induced by rCHI. Analysis of lung microbiome changes revealed an enrichment of lipopolysaccharide (LPS) biosynthesis pathways, suggesting a potential link to neuroprotection. Furthermore, remote PBM mitigated hyperactivation of cortical microglia and astrocytes and significantly reduced excessive synaptic phagocytosis by these cells, highlighting its potential as a preventive strategy for rCHI with neuroprotective effects.

Translational Psychiatry (2025)15:8 ; https://doi.org/10.1038/s41398-025-03228-3

INTRODUCTION

Repeated closed-head injury (rCHI), one of the main types of mild traumatic brain injury (TBI), usually occurs in individuals who are exposed to repeated mild or concussive injury [1]. Multiple impacts in recurrent falls, sports competitions, and traffic accidents are the most common causes of rCHI [1, 2]. As one of the recognized risks for neurodegenerative diseases, rCHI may cause cognitive deficits, motor dysfunction, emotional disorders, and other complications under different conditions [1–3]. Therefore, rCHI prevention and treatment are essential in protecting against or alleviating neurological symptoms in other brain disorders [1–4]. Although a substantial body of studies have been conducted to investigate the pathogenesis and therapeutic strategies, prevention strategies of rCHI remain limited [1].

Neuroinflammation is implicated in various brain diseases, including TBI [5]. In TBI, inflammatory response is essential in primary injury and contributes to the pathological changes in secondary brain injury [2]. For instance, the brain-resident immune cell microglia trigger an inflammatory response by releasing inflammatory cytokines and chemokines and initiate neuroprotective effects by removing cellular debris in response to the primary injury [6]. Moreover, microglia play a key role in synaptic remodeling, where appropriate elimination of redundant synapses is crucial for normal brain development and function [7, 8]. Malfunction in microglial-mediated synaptic pruning has been linked to abnormal behaviors and neurological disorders [7, 8]. Microglia-mediated synaptic pruning involves the interaction between neuronal CD47 and its receptor, Signal Regulatory Protein alpha (SIRPα) [7–9]. CD47 sends a 'don't-eat-me' signal to microglia, inhibiting their phagocytic activity and preventing excessive synaptic elimination during development [8]. This protective function highlights the importance of the SIRPα-CD47 axis in ensuring balanced microglial activity. Recent findings indicate that loss of microglial SIRPα leads to excessive synaptic pruning in neurodegeneration, underscoring its role in synaptic maintenance [8]. In TBI, excessive activation of microglia and a prolonged state of inflammatory response contribute to secondary injury, wherein microglia display significantly elevated synaptic engulfment, causing neuronal damage and behavioral deficits [10]. Moreover, astrocytes, the most abundant glial population in the brain tissue, also respond to brain injury and develop chronic inflammatory responses [11]. Therefore, numerous studies have

[1]Laboratory of Exercise and Neurobiology, School of Physical Education and Sports Science, South China Normal University, Guangzhou 510006 Guangdong, China. [2]Laboratory of Regenerative Medicine in Sports Science, School of Physical Education and Sports Science, South China Normal University, Guangzhou 510006, China. [3]Laboratory of Laser Sports Medicine, School of Physical Education and Sports Science, South China Normal University, Guangzhou 510006, China. ✉email: luodanyang@m.scnu.edu.cn

Received: 22 May 2024 Revised: 13 December 2024 Accepted: 7 January 2025
Published online: 11 January 2025

focused on microglia and astrocytes in the rCHI [1, 2, 4]. However, preventive approaches targeting astrocytes and microglia remain to be explored.

Photobiomodulation, also known as low-level laser therapy, has received tremendous attention for the prevention and treatment of a variety of brain diseases, including ischemic stroke, TBI, mrCHI, Alzheimer's disease (AD), and neonatal hypoxia-ischemia [1, 2, 12–14]. Previous studies have uncovered the effect of PBM in alleviating neuroinflammation by inhibiting excessive microglia activation and promoting the polarization of microglia and astrocytes from pro-inflammatory phenotype to anti-inflammatory phenotype [1, 2, 13–15]. However, the penetration of transcranial PBM to deep tissue penetration ability limits the findings from the preclinical work in animal models to clinical medicine [16]. Intriguingly, in the past several years, remote PBM, referring to the irradiation of tissue to exert beneficial effects on a distant, non-irradiated tissue, has become an emerging therapeutic approach for neuroprotection [16]. Although multiple studies have uncovered the essential role of the lung-brain axis in regulating microglial function and activation states, the effects of remote PBM targeting the lung in preventing rCHI remain unclear [17, 18]. Using a "Marmarou" weight-drop rCHI model and 808 nm continuous wave low-intensity laser, we performed an experiment to explore the effects of remote PBM on rCHI-induced brain injury and behavioral deficits.

METHODS

Animals and experimental design

Sprague-Dawley (SD) rats purchased from the Guangdong Medical Laboratory Animal Center at nine weeks of age were used for the current study, and the animals were allowed to acclimate for one week before the initiation of the experiments. Ten-week-old animals were randomly allocated into the following groups: (1) Control group with Sham PBM (Cont, $n = 9$), (2) Cont animal with remote PBM treatment (Cont+PBM, $n = 9$), (3) rCHI group with Sham remote PBM therapy (rCHI, $n = 10$), and (4) rCHI with remote PBM treatment (rCHI+PBM, $n = 11$). Samples were randomly assigned to experimental groups using a computer-generated randomization method. The investigator was blinded to group allocation throughout the duration of the experiment as well as during the assessment of outcomes. The rCHI animal model was established according to our previous study [1]. As shown in Fig. 1A, an impactor weighing 198.6 g was dropped at a height of 1.2 m to induce a closed-head diffuse traumatic brain injury. To ensure the reproducibility of the Marmarou weight-drop method, we consistently used the same apparatus, weight, and drop height in all injury sessions. The positioning of the animals was carefully standardized to ensure the impact was delivered at the exact anatomical location on the skull across all subjects. Post-injury, animals were closely monitored, and any exhibiting extreme or insufficient behavioral responses (indicating outliers in injury severity) were excluded from the study, thereby minimizing variability in injury outcomes. All procedures were carried out by experienced personnel, and post-injury assessments were blinded to reduce bias. The rCHI animals were subjected to the closed-head diffuse traumatic brain injury on days 0, 5, and 10. The PBM treatment was conducted daily until day 20 (Fig. 1B). Behavioral tests, including the three-chamber social interaction test, grip test, forced swim, open field test, novel object recognition test, and Barnes maze test, were performed, followed by brain tissue collection. All animals were housed in the animal care facility with controlled humidity (~ 50%) and temperature (22–24 °C) under a 12-h day/night cycle. The sample size for this animal study was determined based on prior research findings and the inherent biological variability associated with the selected animal model. All animal experiments in this study were approved by the Animal Ethical and Experimental Committee at South China Normal University and complied with National Institutes of Health (NIH) guidelines. This approval ensured that all procedures adhered to the ethical standards for the care and use of animals.

Remote PBM therapy

Based on our previous studies and preliminary experiments, the remote PBM therapy was conducted using an 808 nm continuous wave low-intensity laser (MDL-III-808-500 mW, Dragon Lasers, Jilin province, China) [14, 15, 19–21]. The 2-min PBM therapy was carried out daily for 20 days with 2 times bilaterally (one time per side) on each animal. A collimated laser beam at 350 mW/cm^2 on the skin surface formed a 2 cm^2 spot area on each side. All rats with or without PBM were shaved every two days before remote PBM therapy. During the remote PBM treatment, all rats were restrained in a transparent *DecapiCone* (DCL-120, Braintree Scientific, Inc., MA). The specific parameters for remote PBM treatment are listed in Supplementary Table 1.

Behavioral tests

Forced swim test. The forced swim test is a widely used behavioral test to examine depressive-like behavior [22]. As described in our previous study, the rats were placed in a tall plastic cylinder (50 cm high × 20 cm diameter) filled with 30 cm-deep water (23 ± 2 °C) for 6 min [23]. The immobile time was recorded and analyzed using an ANY-maze video tracking system.

Grip test. The grip test was carried out to assess the grip strength according to our previous study [20]. A 55-cm metal wire was affixed between two vertical stands and suspended 60 cm above the ground. When gently handled by the tail, each rat was directed to grasp the wire using its forepaws. Once properly suspended, the rat was left to hang autonomously. Hanging wire scores and hanging times were recorded during a 2-min testing period. The hanging wire score, assessed on a 5-point scale, ranged as follows: 0, the rat promptly falls off the wire upon suspension; 1, the rat maintains its initial position by hanging onto the wire with both forepaws; 2, the rat endeavors to climb onto the wire while maintaining a grip with both forepaws; 3, the rat grips the wire with its forepaws while attempting to climb using one or both hind limbs; 4, the rat firmly grasps the wire with both forepaws and hind limbs, additionally wrapping its tail around the wire for support. Three trials were conducted for each animal at 5-min intervals. The highest hanging score and the longest hanging time for each rat were recorded for analysis.

Three-chamber social interaction test. The three-chamber social test is performed to assess sociability and social novelty in animals and is commonly used in studies of social behavior and social anxiety [24]. In the three-chamber social interaction test, each rat was first placed in the central chamber of a three-chamber apparatus to freely explore all chambers for 10 min to habituate to the environment. After habituation, the rat was returned to the central chamber, and one of the side chambers was randomly assigned to contain a conspecific stranger rat (Animal 1) in a wire enclosure. In contrast, the other side chamber remained empty. The rat was then allowed to explore the chambers for 10 min. For the social novelty phase, the rat was returned to the central chamber, Animal 1 was placed in one of the wire enclosures, and a novel conspecific (Animal 2) was placed in the other. The rat was again allowed to explore freely for 10 min, and the interaction with both Animal 1 and Animal 2 was recorded. After testing, the apparatus was cleaned to eliminate olfactory cues, and behavioral data were analyzed.

Open field test. To assess anxiety-like behavior, an open field test was performed following our previous study [19]. The apparatus used in the open field test consisted of a black square box (40 × 60 × 60 cm). Each rat was placed in the center of the arena and allowed to explore freely for 5 min. The time spent in the center zone and the number of fecal boli were automatically recorded using ANY-maze video tracking software. The apparatus was thoroughly cleaned with 70% ethanol between sessions to prevent cross-contamination. The tests were conducted each day during the same period under controlled light and sound conditions.

Elevated plus maze. An elevated plus maze was performed to evaluate anxiety-like behaviors following our previous study [19]. The apparatus was positioned 50 cm above the ground and consisted of two open arms and two closed arms arranged perpendicularly, with a central platform connecting all arms. The closed arms were enclosed by 50-cm-high walls. Each animal was placed in the central platform at the beginning of the trial and allowed to explore the maze for 5 min. The number of entries into the open arms and the duration spent in the open arms were recorded using ANY-maze tracking software. The maze was cleaned with 70% ethanol between trials to avoid scent cues.

Barnes maze task. The Barnes maze task is a widely used assessment for evaluating spatial learning and memory function [25, 26]. A 122-cm-

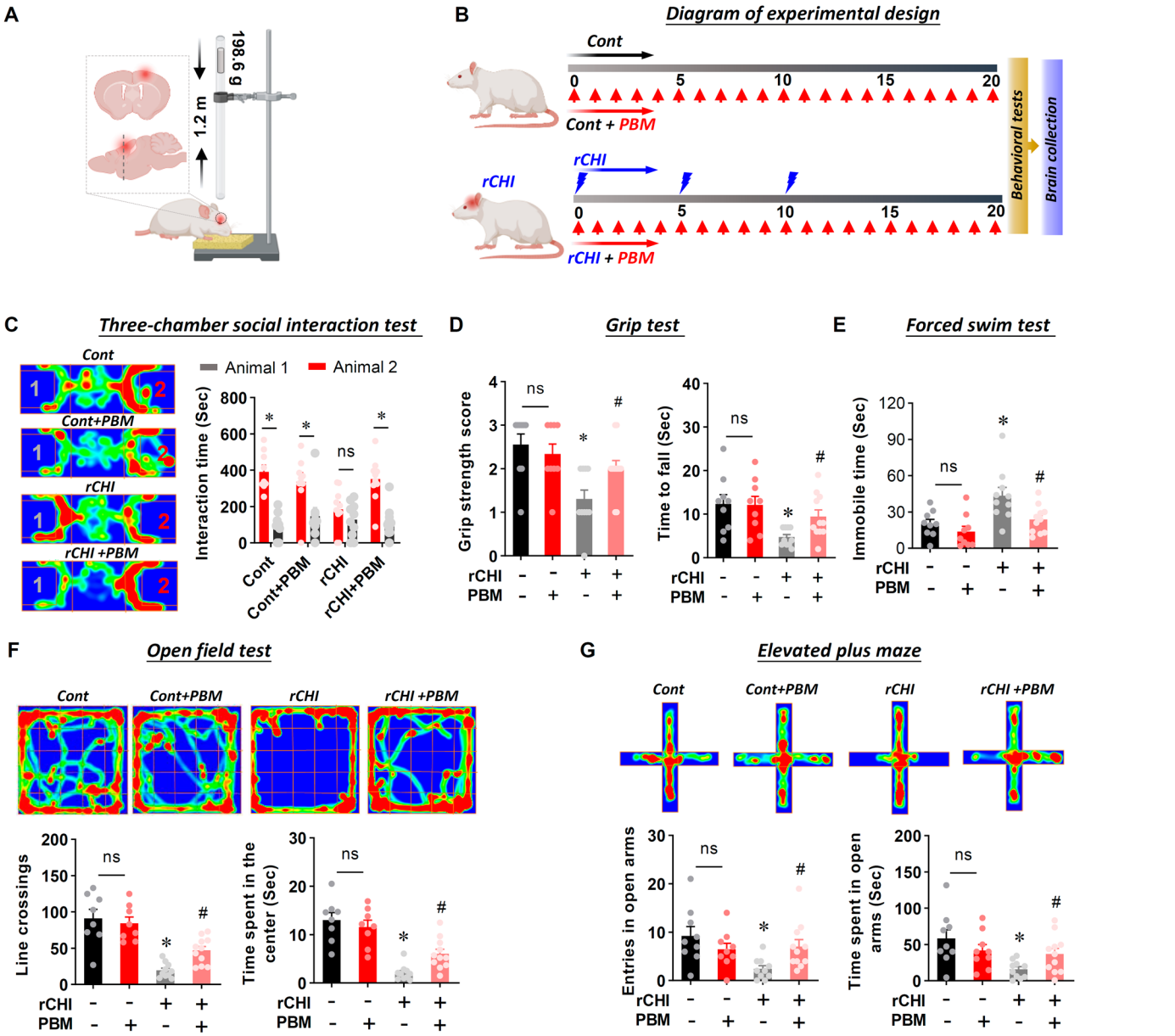

Fig. 1 Experimental design and behavioral outcomes in the rCHI animal model. A Schematic illustration of the rCHI model with a dashed box indicating the damaged area. **B** Diagram of the experimental design outlining the timeline and procedures. **C** Representative images from the three-chamber sociability test, accompanied by statistical analysis of interaction time. **D** Results from the grasping test, including grasping scores and drop latency measurements. **E** Statistical analysis of immobility time during the forced swim test. **F** Representative images from the open field test, along with statistical data online crossings and time spent in the center. **G** Representative images from the elevated plus maze and statistical analysis of entries and time spent in the open arms. Data are presented as mean ± SEM. $^{*}P < 0.05$ versus Cont group, $^{\#}P < 0.05$ versus rCHI group. ns indicates no significant differences.

diameter circular platform with 18 holes around its perimeter and a black escape box hidden under one of the holes was used in the test. The platform was 80 cm from the ground. In brief, the Barnes Maze task was divided into the training trial and the probe test. During the training trials on the first three days, the animals were placed at the center of the circular platform and given 3 min to explore the platform freely. The rats that did not find the escape box within 3 min were gently guided to the target hole. The time spent finding the target hole and entering the escape box was recorded and analyzed. The probe test was carried out on the fourth day and lasted for 90 sec. During the 90-s probe test, the escape box was removed, and the target hole was blocked. During this stage, the circle platform was divided into four quadrants, with one of the quadrants defined as the target quadrant where the escape hole was located. The time staying in the target quadrant was recorded and analyzed using Any-Maze automated video tracking system (Stoelting, Wood Dale, IL, USA).

Novel object recognition (NOR) test. The NOR test evaluated recognition memory with modifications based on our previous study [19]. The test consisted of two phases. In the sampling phase, animals were introduced to two identical objects placed in a rectangular arena (50 × 60 × 60 cm) and allowed to explore for 5 min. Twenty-four hours later, during the choice stage, one of the familiar objects was replaced with a novel object, and animals were again given 5 min to explore the arena. The time spent interacting with each object and movement patterns was tracked and analyzed using ANY-maze video tracking software. The arena and objects were thoroughly cleaned with 70% ethanol between trials to minimize olfactory cues.

Brain collection and tissue preparation

The brain collection was conducted following behavioral tests. As described in our previous study [20], the rats were deeply anesthetized

and transcardially perfused with cold PBS, followed by quick brain collection and post-fixation with 4% paraformaldehyde. The brains were then transferred into 30% sucrose until the brain sank to the bottom. Thereafter, the brain tissue was embedded in OCT and cryosectioned at 25 µm using Leica Rm 2155 microtome. The collected brain slices were stored in an antifreeze solution (PC101, FD NeuroTechnologies, Inc., Columbia, MD).

Immunofluorescence staining

The immunofluorescence staining was conducted as described previously [2, 26, 27]. In brief, the prepared brain slices were permeabilized in 0.4% Triton X-100 for 4 h, followed by blocking with 10% normal donkey serum for another 60 min. Subsequently, the brain slices were incubated overnight with the following primary antibody at 4 °C: anti-NeuN (Sigma, MAB377), MBP (Abcam, ab218011), MAP2 (Abcam, ab5392), synaptophysin (SYP, Sigma, S5768), PSD95 (Invitrogen, 7E3-1B8; Abcam, ab18258), Cleaved-Caspase 3 (Arigo, ARG66671), Cleaved-Caspase 9 (Cell signaling, #9507), GFAP (Abcam, ab4674), Iba-1 (Wako Chemicals, 019-19741), SIRPα (Santa Cruz, sc-376884), and PHF1 (ABclonal, A8450). On the following day, after three washes, the brain slices were incubated with corresponding Alexa Fluor donkey anti-mouse/rabbit/goat second antibodies for 30 min. After the final washes, the brain slices were mounted using DAPI Fluoromount-G® Mounting Medium (SouthernBiotech, 0100-20). Confocal images were captured using an LSM800 confocal laser scanning microscope by an experimenter blinded to the treatment conditions.

TUNEL assay and fluoro-jade C staining

The TUNEL and Fluoro-Jade C staining were carried out to examine cellular apoptosis and degeneration. Neuronal apoptosis was determined by the NeuN/TUNEL double-labeling method, as previously described [25]. A Click-iT® Plus TUNEL with Alexa Fluor®488 assay kit (Thermo Fisher Scientific) was adopted to determine apoptotic cells according to kit instructions. Neurodegeneration was determined by NeuN/Fluoro-Jade C staining. A Fluoro-Jade C (FJC) ready-to-dilute staining kit (TR-100-FJ) was used to identify degenerating neurons following the manufacturer's instructions.

Lung microbiome extraction and 16S rDNA amplicon sequencing

Lung microbiome samples were collected from rats using bronchoalveolar lavage. After euthanizing the rats, a tracheotomy was performed, and a sterile 18 G gavage needle was inserted into the trachea. Pre-warmed PBS (37 °C) was instilled into the lungs and retrieved after 30 s. This step was repeated to obtain an adequate bronchoalveolar lavage fluid (BALF) volume. Total genomic DNA was extracted using the Mag-bind Soil DNA Kit (Omega Bio-Tek), and the DNA concentration and purity were measured. The V3-V4 region of the 16S rRNA gene was amplified using barcoded primers and high-fidelity DNA polymerase. Amplicons were verified by 2% agarose gel electrophoresis and purified using the Quant-iT PicoGreen dsDNA Assay Kit. The PCR products were quantified using the BioTek FLx800 microplate reader system. Libraries were prepared with the TruSeq Nano DNA LT Library Prep Kit (Illumina), and quality was assessed using the Agilent Bioanalyzer 2100 and Promega QuantiFluor. Sequencing was then performed on a high-throughput platform. Functional predictions were analyzed using STAMP and KEGG pathway analysis to identify differences between experimental groups.

Image processing and analysis

Image processing was conducted using Image J (Version 1.49, NIH) or Imaris software (Bitplane AG). The fluorescent intensity was quantified in a blinded manner using Fiji/Image J software. Sholl analysis was performed to analyze the morphology of microglia using Fiji-ImageJ software (Version 2.9.0, NIH) according to previous studies [19, 28]. High-resolution Z-stack images were collected for 3D reconstruction with Imaris software (Bitplane AG), according to our previous study. The spot and surface detection modules were selected according to the demand. When the surface detection module was applied, the surface detail was set at 0.4 µm for all images. The nonspecific signal and background noise were removed by using the appropriate threshold.

Statistical analysis

Data were analyzed using GraphPad Prism Software 8.3.0 or ANY-maze video tracking software (Behavioral tests). Prior to performing statistical comparisons, the assumption of homogeneity of variances was assessed using Levene's test. One-way analysis of variances (ANOVAs) or two-way ANOVA with Student-Newman-Keuls (S-N-K) post hoc was performed to examine the differences among multiple groups. Significance was determined with Student's *t*-test (two-tailed) for two group comparisons. All data were expressed as means ± SEM. *P*-values less than 0.05 were considered statistically significant.

RESULTS

Remote PBM ameliorates rCHI-induced depressive-like behavior, motor deficits, and social interaction impairment

We first explored the effects of remote PBM on rCHI-induced behavioral changes using various tests. The three-chamber social interaction test (Fig. 1C) showed that rCHI animals did not exhibit a significant difference in interaction time with Animal 1 (familiar rat) and Animal 2 (novel rat), indicating an impairment in social interaction. However, remote PBM targeting the lung significantly increased the interaction time with Animal 2, suggesting that remote PBM improved the social interaction deficits induced by rCHI. As shown in Fig. 1D, the grip test results revealed that rCHI led to significant motor deficits, as evidenced by a decreased grip strength score and time to fall. In contrast, remote PBM therapy significantly improved grip strength and time to fall, indicating that it effectively ameliorated the rCHI-induced motor deficits. In the forced swim test (Fig. 1E), rCHI animals displayed a significantly increased immobile time compared to control animals, indicating depressive-like behavior induced by rCHI. Interestingly, remote PBM targeting the lung significantly reduced the immobile time, suggesting that remote PBM alleviates rCHI-induced depressive-like behavior. In the open field test (Fig. 1F), rCHI animals demonstrated a significant reduction in the number of line crossings and the time spent in the center of the field, indicative of anxiety-like behavior. Remarkably, remote PBM therapy reversed these changes, significantly increasing both line crossings and time spent in the center, reflecting a reduction in anxiety-like behavior. Similarly, the elevated plus maze test (Fig. 1G) showed that rCHI animals exhibited a significantly reduced number of entries and time spent in the open arms, suggesting increased anxiety. Remote PBM therapy significantly alleviates these changes, increasing the number of open-arm entries and time spent in the open arms, demonstrating the anxiolytic effects of remote PBM in rCHI animals.

In contrast, the results of the Barnes maze test (Supplementary Fig. 1A), which assesses spatial memory, revealed that rCHI did not induce significant changes in escape latency or quadrant occupancy. This finding indicates that rCHI does not affect spatial memory, and remote PBM therapy did not significantly alter these results. Likewise, the NOR test (Supplementary Fig. 1B), used to evaluate recognition memory, showed no significant differences in preference for exploring the novel object following rCHI insults and remote PBM treatment. This finding suggests that rCHI did not impair recognition memory, and remote PBM did not produce notable changes in this task.

Remote PBM protects against rCHI-induced neuronal damage, apoptosis, and neurodegeneration

We next sought to investigate the effects of remote PBM on neuronal damage, apoptosis, and neurodegeneration. Firstly, MAP2, MBP, synaptophysin (SYP, presynaptic marker), and PSD-95 (postsynaptic marker) staining were conducted to analyze neuronal damage following rCHI insults and remote PBM therapy. As shown in Fig. 2A(a, b), rCHI caused remarked MAP2 fragmentation in the cortex, as evidenced by significantly increased small particles and reduced continuous structure. In contrast, remote PBM protects against rCHI-induced MAP2 fragmentation in the cortex. In line with this finding, the MAP2 dispersion was significantly increased compared with the control

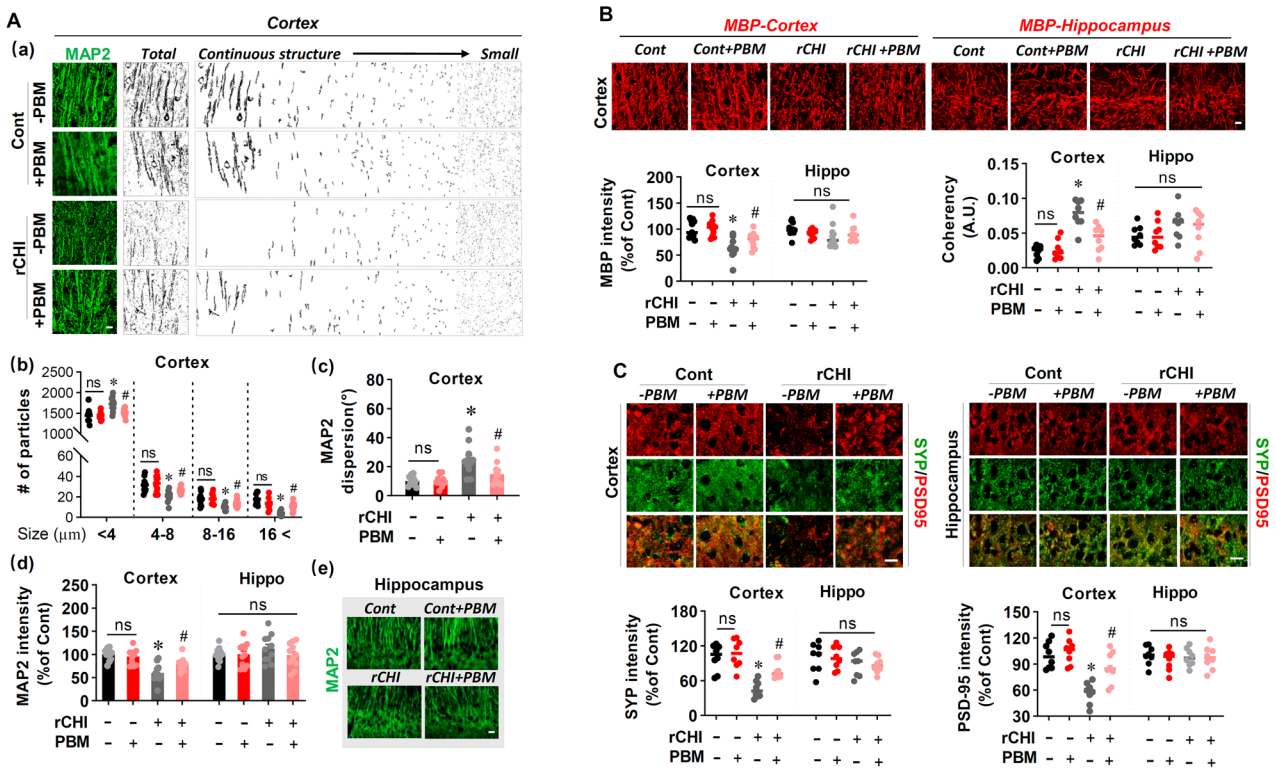

Fig. 2 Remote PBM ameliorates neuronal damage caused by rCHI. A Representative immunofluorescence images of MAP2 in the cortex (a). MAP2 fragments were divided into continuous structures and fragmented structures of varying sizes. Quantitative analysis of the number of particles of different sizes (b). Statistical analysis of MAP2 dispersion (c). Statistical analysis of MAP2 fluorescence intensity (d). Representative immunofluorescence images of MAP2 in the hippocampus (e). **B** Representative immunofluorescence images of MBP, including analyses of immunofluorescence intensity and coherency. **C** Representative immunofluorescence images of presynaptic and postsynaptic proteins, along with the analysis of immunofluorescence intensity. Scale bar = 10 μm. Data are presented as mean ± SEM. $^{*}P < 0.05$ versus Cont group, $^{\#}P < 0.05$ versus rCHI group. ns indicates no significant differences.

and rCHI animals (Fig. 2A(c)). Moreover, animals in the rCHI group presented a decreased MAP2 intensity in the cortex, which was alleviated by remote PBM (Fig. 2A(d)). No significant changes in the MAP2 intensity in the hippocampus were detected (Fig. 2A(d, e)). Furthermore, as shown in Fig. 2B, C, MBP, SYP, and PSD-95 staining showed that rCHI induced a remarkedly reduced intensity in the cortex compared with control animals. However, remote PBM attenuated this decrease in the cortex of the rCHI animals. Analysis of the coherency of MBP confirmed the neuroprotective effects of remote PBM therapy following rCHI insults, as evidenced by significantly increased coherency in the rCHI group and reduced coherency in the remote PBM group (Fig. 2B). Notably, no neuronal injury was observed in the hippocampus following rCHI exposure.

Next, the neuronal apoptosis was analyzed by co-staining NeuN with TUNEL and cleaved-caspase 3/9. As shown in Fig. 3A, rCHI induced significantly increased TUNEL-positive neurons compared to the control and rCHI animals with remote PBM therapy. Moreover, rCHI caused significantly increased cleaved-caspase-3 and caspase-9 levels compared to control animals and remoted PBM-treated rCHI animals, which further confirmed that remote PBM alleviated rCHI-induced neuronal apoptosis (Fig. 3B, C).

Subsequently, Fluro-Jade C staining was conducted to assess neurodegeneration following rCHI and remote PBM therapy. As shown in Fig. 3D, rCHI induced a markedly increased neuronal degeneration in the cortex compared with the control animals, as evidenced by significantly elevated Fluro-Jade C-positive neurons. In contrast, rCHI animals with remote PBM therapy displayed significantly decreased Fluro-Jade C-positive neurons, suggesting that remote PBM therapy alleviates rCHI-induced neurodegeneration. No Fluro-Jade C-positive neurons were detected in the hippocampus.

Remote PBM alleviates excessive activation of glial cells

Excessive activation of glial cells is one of the crucial pathological changes in brain injury, contributing to neuronal apoptosis and degeneration [1]. Therefore, we then analyze the changes in glial cells following rCHI and remote PBM therapy. As shown in Fig. 4A, rCHI caused significantly elevated GFAP intensity in the cortex compared to the Cont animal. In contrast, the elevated GFAP intensity in the cortex of the rCHI animal was attenuated following remote PBM therapy. In addition, the astrocytes in the cortex of the rCHI animals became hypertrophy, and the processes became longer, suggesting excessive activation of the astrocytes. 3D reconstruction of the astrocyte with different colors representing different cellular volumes. 3D rendering analysis confirmed the increased astrocyte volume in the cortex of the rCHI animals and the alleviation following remote PBM therapy (Fig. 4B).

Similar changes were obtained in the microglia following rCHI and remote PBM therapy. As shown in Fig. 4C, rCHI caused a significant increase in Iba-1 intensity, which was attenuated by the PBM therapy. Moreover, the Sholl analysis was conducted to analyze the morphological changes of microglia with concentric circles to the cell body (Fig. 4D(a)). The microglia in the cortex of the rCHI animal exhibited markedly decreased intersection numbers with the circles compared with the Cont animals (Fig. 4D(b)). Interestingly, remote PBM ameliorated the decrease in intersection number with the concentric circles (Fig. 4D(b)). No significant changes were observed in the intersection number with the concentric circles in the hippocampus among groups (Fig. 4D(c)). Moreover, further analysis found that rCHI induces significant reductions in branch length (Fig. 4D(d)), maximum branch length (Fig. 4D(e)), number of branches (Fig. 4D(f)), and mean interaction (Fig. 4D(g)), and significantly increased solidity (Fig. 4D(h)), and microglial cell body

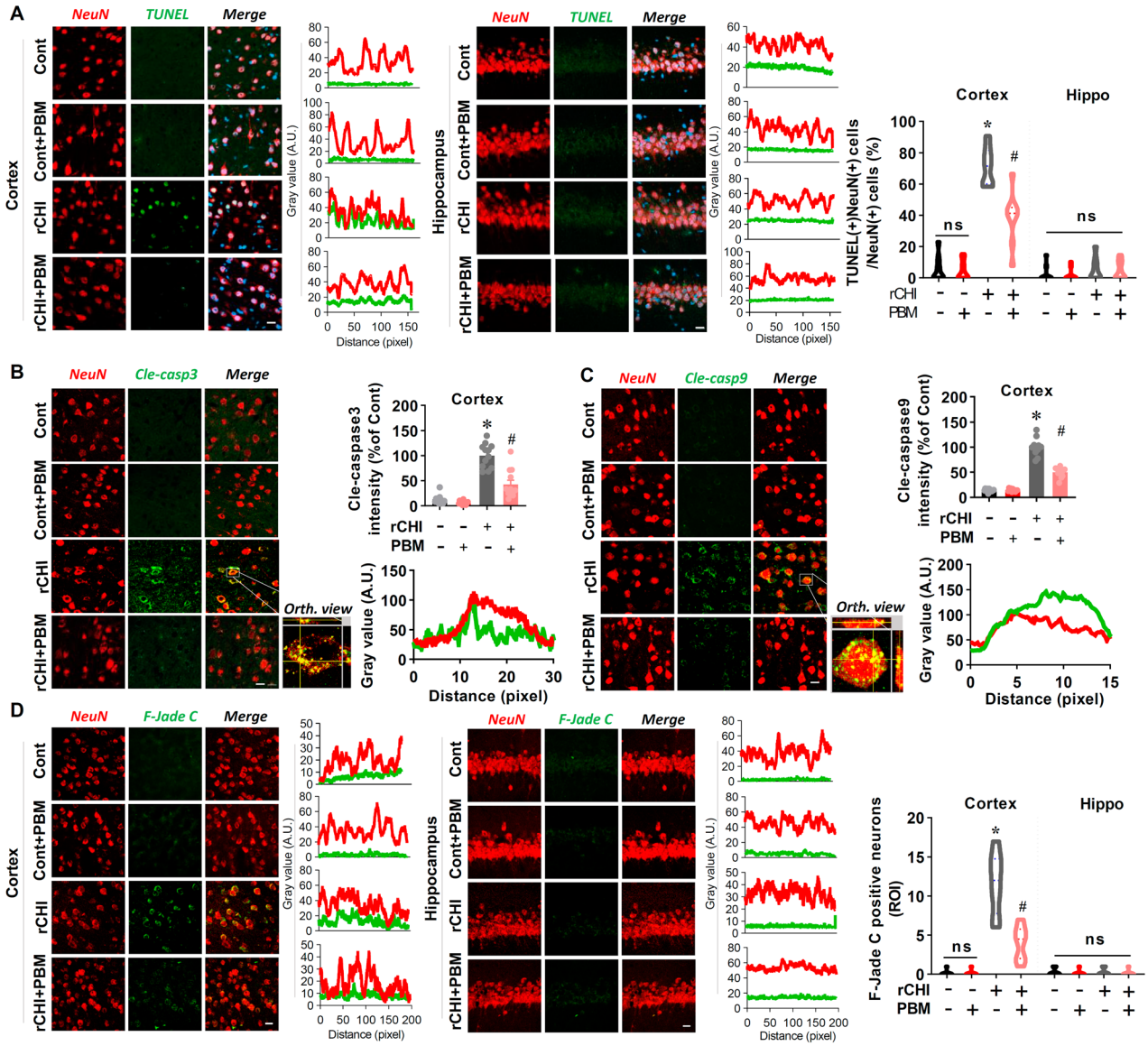

Fig. 3 Remote PBM ameliorates neuronal apoptosis and degeneration caused by rCHI. A Representative immunofluorescence images of co-staining of NeuN and TUNEL. Line-scan analysis was utilized to assess co-localization. Statistical analysis depicting the number of TUNEL and NeuN positive cells in the cortex and hippocampus. **B** Representative immunofluorescence images showing co-staining of NeuN and cleaved-caspase 3. Co-localization analysis of NeuN and cleaved-caspase 3 and statistical quantification of cleaved-caspase 3 immunofluorescence intensity. **C** Representative immunofluorescence images demonstrating co-staining of NeuN and cleaved-caspase 9. Co-localization analysis of NeuN and cleaved-caspase 9 and statistical quantification of cleaved-caspase 9 immunofluorescence intensity. **D** Representative immunofluorescence images displaying co-staining of NeuN and Fluoro-Jade C. Co-localization analysis of NeuN and Fluoro-Jade C and the number of Fluoro-Jade C-positive neurons. Scale bar = 10 μM. Data are presented as mean ± SEM. $^{*}P < 0.05$ versus Cont group, $^{\#}P < 0.05$ versus rCHI group. ns indicates no significant differences. AU arbitrary unit.

diameters (Fig. 4D(i)) in the cortex. By contrast, remote PBM attenuates rCHI-induced morphological changes of microglia in the cortex. Notably, no morphological changes of microglia in the hippocampus were observed.

Remote PBM attenuates excessive synapse elimination by microglia and astrocytes

Excessive synapse elimination by microglia and astrocytes following brain injury and neurodegeneration is involved in the disease development [29, 30]. Therefore, we examine the effects of rCHI and remote PBM on synapse elimination. As shown in Fig. 5A, the 3D reconstruction of representative co-staining images of Iba-1 and PSD95 (a postsynaptic marker) confirmed the excessive synapse elimination by microglia in the cortex of the rCHI animals, which was significantly ameliorated by remote PBM. Similarly, 3D-rendered images of the co-staining of GFAP and PSD95 observed increased PSD95 puncta within astrocytes in the cortex of the rCHI animals (Fig. 5B), suggesting that rCHI caused excessive synapse elimination by astrocytes. Remote PBM alleviates excessive synapse elimination. Notably, there were no significant differences in the hippocampus between groups.

Remote PBM preserves microglial SIRPα and inhibits tau pathology

Microglial SIRPα and tau pathology are essential signals in glial-mediated excessive synapse elimination [8, 31]. We then analyzed the effects of rCHI and remote PBM on microglial SIRPα and p-tau in the cortex and hippocampus. As shown in Fig. 6A, 3D-rendered

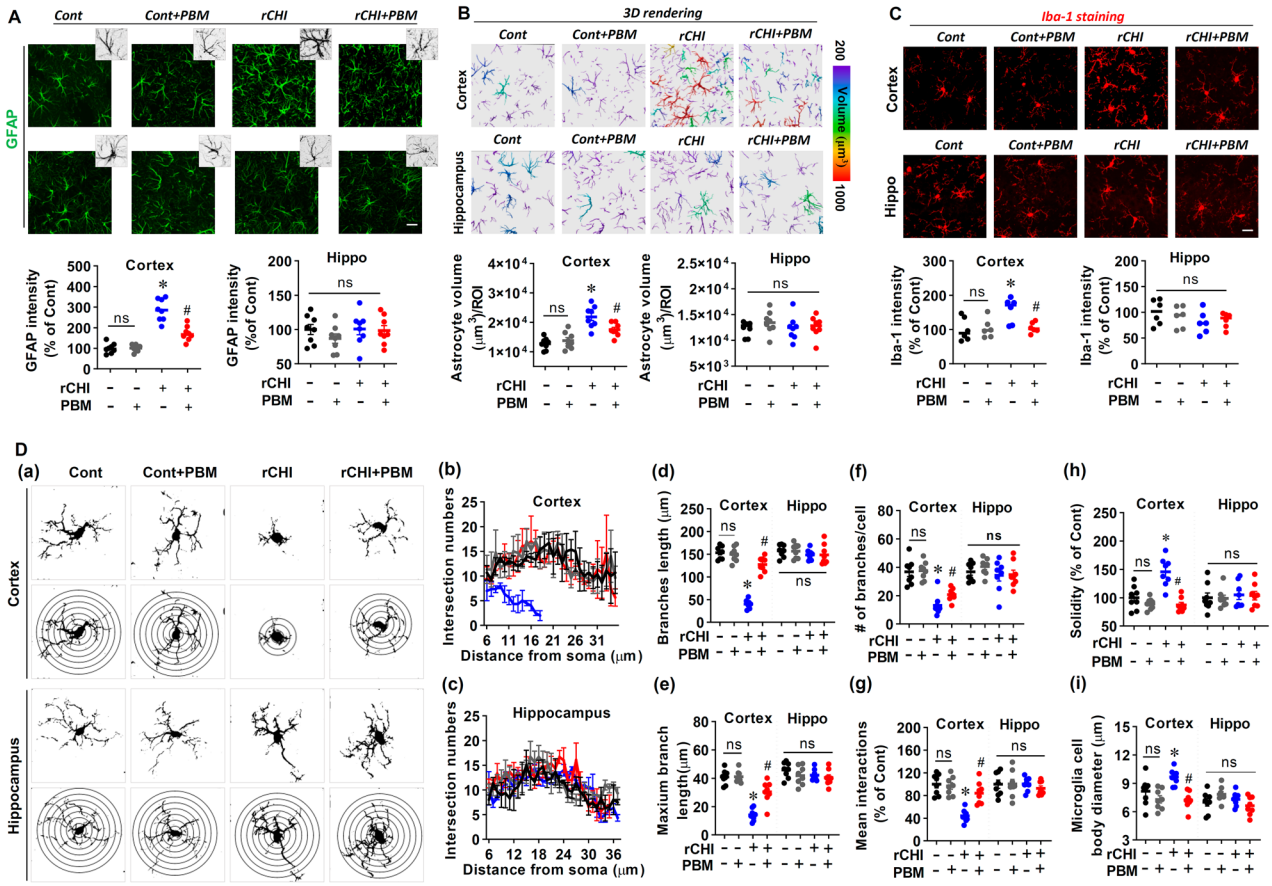

Fig. 4 Remote PBM alleviates excessive activation of microglia and astrocytes. A Representative immunofluorescence image of GFAP staining. An enlarged view of the area was shown in the upper right corner of the images. Statistical analysis of GFAP immunofluorescence intensity in the hippocampus and cortex is shown as a percentage of control. **B** 3D reconstruction of GFAP immunofluorescence images and analysis of astrocyte volume. **C** Typical representative images showing Iba-1 immunofluorescence staining of microglia, with statistical analysis of Iba-1 immunofluorescence intensity. **D** Typical representative images of Sholl analysis of microglia (a). The number of intersections (b and c), branch length (d), maximum branch length (e), branch number per cell (f), mean interactions (g), solidity (h), and microglial cell body diameter (i) were analyzed. Data are presented as mean ± SEM. $^{*}P < 0.05$ versus Cont group, $^{\#}P < 0.05$ versus rCHI group. ns indicates no significant differences. ROI region of interest.

images showed that rCHI induced significantly decreased levels of microglial SIRPα compared to the control rats. Intriguingly, remote PBM preserves microglial SIRPα in the cortex of the rCHI animals. Next, we measured the effects of rCHI and remote PBM on p-tau. As shown in Fig. 6B, rCHI induced increased tau phosphorylation, and remote PBM ameliorated these changes.

Remote PBM modulates lung microbiome composition and enhances lipopolysaccharide biosynthesis pathways

To investigate the potential mechanisms by which remote PBM targeting the lung improves rCHI-induced brain injury and behavioral deficits, we performed 16S rDNA amplicon sequencing to analyze the lung microbiome. At the phylum level, we observed a significant increase in several bacterial phyla following remote PBM treatment, including Bacteroidetes (Supplementary Fig. 2A). Further analysis of the *Bacteroidetes* phylum revealed increases in specific bacterial families, including *Prevotellaceae, Muribaculaceae*, and *Rikenellaceae* (Supplementary Fig. 2B). Moreover, functional analysis using STAMP (Statistical Analysis of Metagenomic Profiles) was performed to compare the functional abundance between the rCHI and rCHI+PBM groups. The KEGG (Kyoto Encyclopedia of Genes and Genomes) pathway analysis from the STAMP results indicated a significant enrichment in pathways related to lipopolysaccharide biosynthesis in the rCHI+PBM group compared to the rCHI group.

DISCUSSION

Our study demonstrated that remote PBM targeting the lung effectively alleviated rCHI-induced depressive-like behavior, motor deficits, and social interaction impairments, significantly reducing neuronal damage, apoptosis, and degeneration. Further investigations revealed that remote PBM attenuated rCHI-induced excessive activation of microglia and astrocytes, thereby ameliorating excessive synapse elimination driven by these glial cells. Additionally, we confirmed that remote PBM preserves microglial SIRPα levels and inhibits tau pathology, which may contribute to the reduced excessive synapse elimination in the cortex following rCHI. Importantly, we also observed significant alterations in the lung microbiome following remote PBM treatment, indicating a potential link between lung microbiota modulation and neuroprotection. This is the first study to demonstrate the neuroprotective effects of remote PBM based on the lung-brain axis in regulating microglial function, which may facilitate further investigations of remote PBM targeting the lung in other brain diseases.

Chronic traumatic encephalopathy (CTE) is a progressive neurodegenerative disease associated with repetitive brain injuries, including rTBI, which frequently occurs in high-contact sports (e.g., ice hockey, boxing, soccer), high-risk activities (e.g., skiing, off-road cycling), military combat, and traffic accidents [1, 2, 32, 33]. Although rCHI is a high-risk factor for

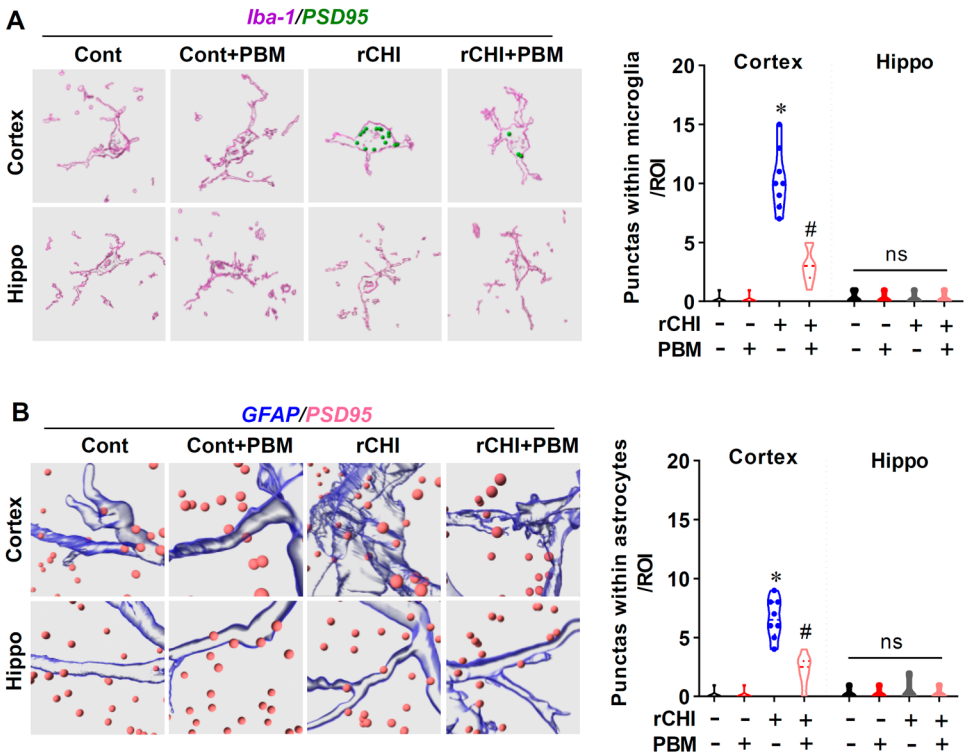

Fig. 5 Remote PBM attenuates excessive synapse elimination by microglia and astrocytes. A 3D reconstruction of immunofluorescence images of Iba-1/PSD95; **B** 3D reconstruction of immunofluorescence images of GFAP/PSD95. Punctas within microglia and astrocytes were analyzed and quantified. Data are presented as mean ± SEM. $^{*}P < 0.05$ versus Cont group, $^{\#}P < 0.05$ versus rCHI group. ns indicates no significant differences. ROI region of interest.

neurodegenerative diseases and psychiatric disorders, it is often challenging to diagnose until irreversible brain damage occurs [34, 35]. Preventive strategies are therefore necessary to mitigate both short- and long-term neurological consequences.

Our previous studies found that rCHI-induced motor coordination deficits, reduced locomotor activity, and anxiety-like behaviors [2, 4]. In this study, using the "Marmarou" weight-drop model, an animal model that could effectively simulate aspects of rTBI, such as repeated concussive impacts, behavioral deficits, neuroinflammation, and tau hyperphosphorylation, we confirmed that rCHI could induce anxiety-like behaviors and impair motor coordination, reflected in a decrease in grip strength. Intriguingly, the behavioral changes induced by rCHI were alleviated by remote PBM. Notably, the remote PBM therapy was initiated following the first "hit" and was conducted daily during the establishment, suggesting remote PBM may serve as a potential strategy for rCHI prevention. Although the "Marmarou" weight-drop model does not fully replicate the chronic and progressive nature of CTE, the beneficial effects of PBM on CTE were demonstrated in treating CTE in human patients [36]. These findings on the therapeutic effects of remote PBM treatment for rCHI, combined with prior research on PBM's benefits for CTE, underscore its potential as a versatile intervention for both acute traumatic injuries and chronic neurodegenerative conditions, including CTE.

Moreover, our earlier research indicated behavioral improvements in the elevated plus maze and open field tests following transcranial PBM treatment in rCHI [2]. In the current study, we found that remote PBM targeting the lungs enhances the results in these tests and significantly improves outcomes in the forced swim, grip, and three-chamber sociability tests. Although remote PBM appears to yield greater behavioral improvements, we cannot conclusively determine its superiority over transcranial PBM solely based on these findings, as such a comparison must take into account differences in treatment parameters. In this study, remote PBM involved a total irradiation time of 4 min (2 min per lung side), which contrasts with the multiple sessions of transcranial PBM previously employed. Furthermore, the effectiveness of PBM is influenced by various parameters, such as irradiation duration, wavelength, and treatment area [37]. Without fully optimizing these parameters for each treatment site, it is challenging to determine whether remote PBM targeting the lungs is more effective than direct brain irradiation. However, it is essential to note that both remote PBM in the current study and transcranial PBM in our earlier research have demonstrated significant behavioral improvements in mitigating impairments caused by rCHI [2]. These findings suggest that in future studies, it would be valuable to compare remote PBM and transcranial PBM after optimizing the treatment parameters for both approaches.

Additionally, the current study observed rCHI-induced neuronal apoptosis, damage, and degeneration [1, 2, 4, 38]. Intriguingly, we observed that rCHI-induced changes were significantly alleviated following remote PBM therapy, suggesting remote PBM could protect neurons against rCHI. In terms of mechanisms, we identified significant alterations in the lung microbiome post-remote PBM treatment, indicating a potential link between lung microbiota modulation and neuroprotection. Specifically, targeting the lung with remote PBM resulted in substantial changes in the lung microbiota composition, particularly an increase in the bacterial phylum *Bacteroidetes*. Within this phylum, families such as *Prevotellaceae, Muribaculaceae*, and *Rikenellaceae* exhibited significant increases. This finding aligns with previous studies suggesting that microbiota composition can influence neuroinflammatory responses and overall brain health [17]. Functional analysis using STAMP revealed significant enrichment in pathways related to LPS biosynthesis in the following remote PBM treatment. This is particularly relevant, as it correlates with existing literature indicating that local treatments can shift microbiota toward LPS-enriched phyla, impacting brain-resident microglial

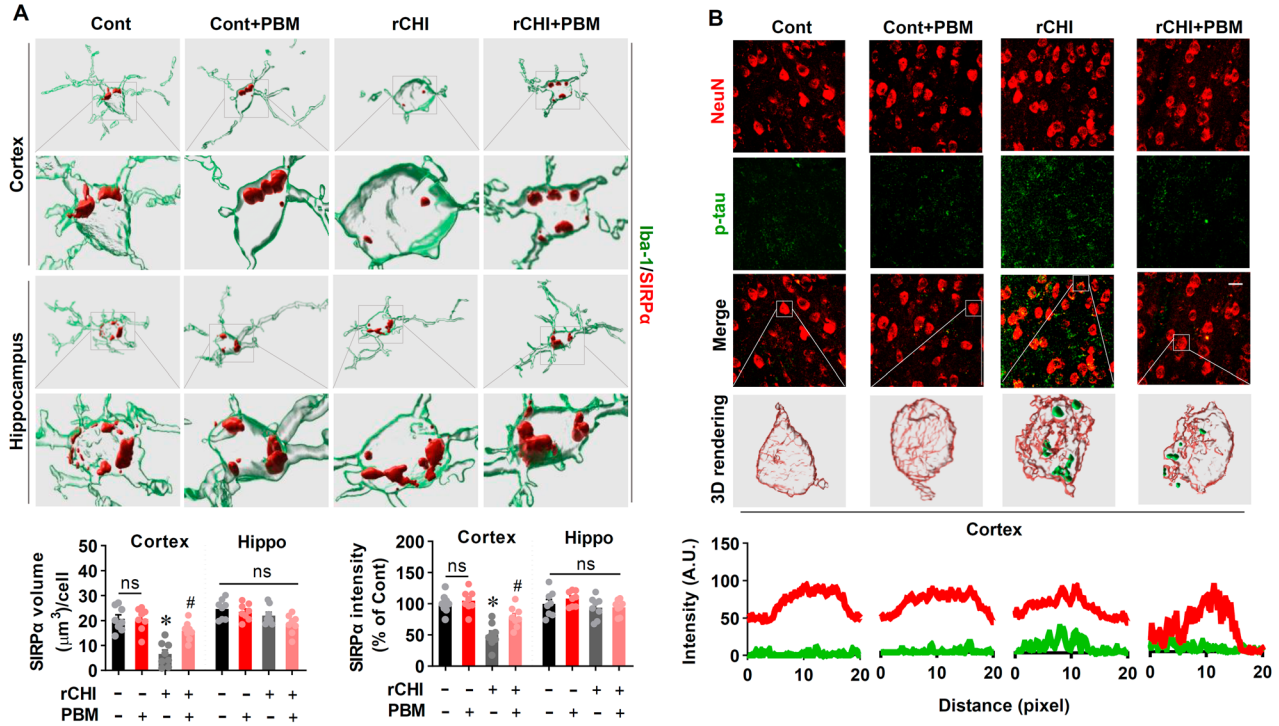

Fig. 6 Remote PBM preserves microglial SIRPα and inhibits tau pathology. A 3D-rendered images of Iba-1 and SIRPα. The volume of the SIRPα and intensity were analyzed. **B** Representative confocal images showed NeuN (red) and p-tau (green) fluorescent signals in the cortex and hippocampus. The co-localization of p-tau and NeuN signals was analyzed by using a line-scan analysis. Scale bar = 10 μm. Data are presented as mean ± SEM. *$P < 0.05$ versus Cont group, #$P < 0.05$ versus rCHI group. ns indicates no significant differences. AU arbitrary unit.

cells [17]. Specifically, according to the previous study, such microbiota alterations may prime microglia towards a type-I interferon state, impairing their responsiveness to autoimmune stimuli from type-II interferons [17]. This impairment is thought to reduce pro-inflammatory responses and associated clinical symptoms, further emphasizing the intricate relationship between microbiota modulation and neuroinflammatory changes in the context of neuroprotection [17].

Consistent with the earlier statement, neuroinflammation plays a significant role in rCHI [1, 2, 4, 38]. Microglia, in particular, is crucial in this process [1, 2, 4, 38]. Therefore, regulating the activation state of microglia could potentially impact the pathological progression of rCHI [1, 2, 4, 38]. Existing research has established the crosstalk between the lungs and the brain [17, 18, 39]. For instance, as mentioned earlier, a previous study has found that changes in the lung microbiome can affect the immune function of microglia in brain tissue [17]. Therefore, in the current study, remote PBM was performed by targeting the lungs to investigate its effects on microglia following rCHI. Exhilaratingly, rCHI-induced excessive activation of microglia in the cortex was attenuated by remote PBM. Generally, microglial activation could induce the excessive activation of astrocytes [40]. Consistent with the changes in microglia, rCHI-induced excessive activation of astrocytes was alleviated following remote PBM therapy. These findings suggest that remote PBM targeting the lungs could alleviate neuroinflammation, contributing to the neuroprotective effects of remote PBM. It is critical to note, however, that accumulating evidence indicates that PBM can stimulate neurogenesis by modulating the inflammatory environment and reducing oxidative stress, both of which are critical for the regeneration of neurons in the hippocampus and other brain regions affected by injury [15, 41, 42]. This suggests that the neuroprotective effects observed in our study may not only be due to the reduction of neuroinflammation but also potentially involve enhanced neurogenesis. Therefore, further exploration is needed to determine whether remote PBM targeting the lungs directly facilitates neurogenesis.

In addition to neuroinflammation, microglia-mediated synaptic engulfment is another crucial factor determining the severity of brain injury and recovery following stroke [43]. Although microglial phagocytosis is essential in alleviating neuroinflammation by clearing cellular debris, excessive microglial synaptic engulfment exacerbates neuronal damage and loss [43, 44]. A previous study has found that inhibition of microglia-mediated excessive engulfment could improve post-stroke functional recovery, suggesting that regulating microglia-mediated synaptic engulfment has the potential to alleviate brain injury [44]. In the current study, we observed significantly increased microglia-mediated synapse engulfment, suggesting rCHI could induce synapse loss and injury. In contrast, remote PBM significantly alleviates excessive microglial synaptic engulfment, supporting the neuroprotective effects of remote PBM targeting the lungs. In light of this result, we should also note that in addition to reducing excessive synaptic engulfment, PBM has been shown to stimulate synaptogenesis, thereby promoting the formation of new synaptic connections [45, 46]. This synaptogenic effect of PBM may further contribute to its neuroprotective potential by compensating for synaptic loss and supporting neural circuit repair following injury. PBM can enhance synaptic plasticity by modulating key factors involved in synapse formation and stability, such as brain-derived neurotrophic factor (BDNF) and synapsin [45, 46]. Therefore, the observed reduction in microglia-mediated synapse elimination in our study may be accompanied by an increase in synaptogenesis, which could potentially enhance recovery from rCHI-induced synaptic loss; however, further studies are still needed to confirm this. Moreover, astrocytes were also involved in synapse elimination, contributing to the development of neurological disease [47]. Like microglia, we found that rCHI induced excessive astrocytes-mediated excessive engulfment, which is ameliorated by remote PBM.

Microglial SIRPα, an essential protein in the "do not eat me" signal, is crucial in protecting synapses from excessive elimination [8, 48]. Loss of SIRPα caused synapse loss and exacerbated neurological pathology in multiple brain diseases [8, 48, 49]. SIRPα interacts with CD47 on the surface of neurons, providing a protective signal that inhibits microglial phagocytosis of healthy synapses [7–9]. In the current study, we detected decreased microglial SIRPα following rCHI and preserved SIRPα in the remote PBM-treated animals, which fit well with the changes in microglia-mediated synaptic engulfment. This preservation of SIRPα may be a key mechanism through which remote PBM reduces synapse loss and promotes neuroprotection in the cortex after rCHI. Furthermore, previous studies have found increased tau hyperphosphorylation following rCHI insults, and tau pathology serves as an essential signal in glial-mediated excessive synapse elimination [1, 8, 31]. Consistent with previous findings, p-tau was significantly increased in the rCHI group, but remote PBM treatment effectively mitigated this increase, further supporting the notion that remote PBM may attenuate tau-related changes through the preservation of microglial SIRPα and inhibition of tau pathology.

In addressing the challenges associated with rCHI, remote PBM was administered starting on day 1 following the initial head injury, enabling the exploration of its efficacy as an early intervention. This design allowed for assessing PBM's impact on mitigating the progression of neuroinflammation, synaptic damage, and behavioral deficits associated with repeated injuries. However, it should be noted that in clinical scenarios, patients are unlikely to seek treatment immediately after a single injury, often waiting until after multiple concussions and the onset of symptoms. As such, PBM would typically be applied later in the injury process. While our study demonstrates the benefits of early intervention, we believe PBM may also hold therapeutic potential even when initiated after several head injuries. The ability of PBM to reduce microglial and astrocyte hyperactivation and prevent excessive synaptic elimination suggests it could mitigate the cumulative damage associated with rTBI. Future studies should focus on delayed PBM application to better simulate clinical treatment timelines and evaluate its therapeutic efficacy after multiple injuries. It is important to note that the findings suggest PBM may serve as a potential routine preventive intervention for athletes engaged in high-risk sports, such as rugby or football, where repeated head trauma is prevalent. Incorporating regular PBM sessions into post-game recovery protocols, akin to relaxation exercises or physiotherapy, could help prevent the cumulative effects of head injuries over time. The non-invasive and simple nature of PBM makes it a feasible and accessible option for athletes, even before symptoms manifest.

Furthermore, while this study primarily investigates the lung-brain axis as a potential mechanism underlying the neuroprotective effects of remote PBM, it is acknowledged that systemic mechanisms may also play a significant role. Previous research has indicated that PBM, even when administered to regions not directly influencing the brain, can elicit systemic effects that enhance brain function [50–55]. These mechanisms may involve modifications in peripheral immune responses, mitochondrial activity, or improvements in circulatory function, as suggested by other studies focusing on brain injury and neurodegeneration [50–55]. Nevertheless, the findings of this study do not exclude the possibility that these systemic effects may interact synergistically with the lung-brain axis to produce the observed neuroprotection.

Moreover, remote PBM offers a significant advantage over traditional drug therapies due to its non-invasive and non-pharmacological nature, which mitigates risks such as drug-related side effects, toxicity, and interactions. While traditional therapies can struggle with issues like crossing the blood-brain barrier and long-term adverse effects, remote PBM has a favorable safety profile with minimal side effects and no tissue damage from non-ionizing light [19, 37]. Although this study highlights remote PBM's potential in modulating lung-to-brain signaling, further long-term research is needed to evaluate its safety. To the best of our knowledge, no studies have specifically investigated the long-term effects of remote PBM targeting the lungs and its regulatory impact on the brain. However, existing literature on PBM, particularly with low-level lasers, reports no adverse effects [19, 56]. For instance, our previous study showed no adverse outcomes after applying PBM for 2 min, three times weekly, over 16 months in transgenic AD [19]. Despite the lack of adverse findings, additional research is vital to explore the potential long-term effects of remote PBM, especially when targeting both the lungs and brain. Understanding these factors is essential for the future development and clinical application of PBM.

In conclusion, our study demonstrated that remote PBM exerts neuroprotective effects, at least partially, by modulating the lung-brain axis. The potential mechanisms underlying the neuroprotective effects of remote PBM may include the alleviation of neuroinflammation by regulating the activation of microglia and astrocytes and the attenuation of microglia-/astrocytes-mediated excessive synaptic engulfment by modulating microglial SIRα and tau pathology. Overall, these findings demonstrated remote PBM targeting the lung could potentially prevent rCHI-induced brain injury and behavioral deficits and advance our understanding of remote PBM by, at least partially, targeting the "lung-brain" axis. Future research should further elucidate the relative contributions of systemic mechanisms and the lung-brain axis to better optimize PBM for clinical use in preventing and treating brain injuries.

DATA AVAILABILITY

All major data supporting the findings of this study are available within the article and its supplementary files. Raw data supporting the findings are available from the authors upon reasonable request.

REFERENCES

1. Yang B, Xu J, Li Y, Dong Y, Li Y, Tucker L, et al. Photobiomodulation therapy for repeated closed head injury in rats. J Biophoton. 2020;13:e201960117.
2. Chen Z, Li M, Wu C, Su Y, Feng S, Deng Q, et al. Photobiomodulation therapy alleviates repeated closed head injury-induced anxiety-like behaviors. J Biophoton. 2024;17:e202300343.
3. Flerlage WJ, Langlois LD, Rusnak M, Simmons SC, Gouty S, Armstrong RC, et al. Involvement of lateral habenula dysfunction in repetitive mild traumatic brain injury-induced motivational deficits. J Neurotrauma. 2023;40:125–40.
4. Xiong J, Lv Y, Ma X, Peng G, Wu C, Hou J, et al. Neuroprotective effect of sublethal hyperthermia preconditioning in a rat model of repeated closed head injury. Neuroscience. 2023;522:57–68.
5. van Erp IAM, Michailidou I, van Essen TA, van der Jagt M, Moojen W, Peul WC, et al. Tackling neuroinflammation after traumatic brain injury: complement inhibition as a therapy for secondary injury. Neurotherapeutics. 2023;20:284–303.
6. Karve IP, Taylor JM, Crack PJ. The contribution of astrocytes and microglia to traumatic brain injury. Br J Pharmacol. 2016;173:692–702.
7. Cornell J, Salinas S, Huang HY, Zhou M. Microglia regulation of synaptic plasticity and learning and memory. Neural Regen Res. 2022;17:705–16.
8. Ding X, Wang J, Huang M, Chen Z, Liu J, Zhang Q, et al. Loss of microglial SIRPalpha promotes synaptic pruning in preclinical models of neurodegeneration. Nat Commun 2021;12:2030.
9. Lehrman EK, Wilton DK, Litvina EY, Welsh CA, Chang ST, Frouin A, et al. CD47 protects synapses from excess microglia-mediated pruning during development. Neuron. 2018;100:120–34.e6.
10. Krukowski K, Nolan A, Becker M, Picard K, Vernoux N, Frias ES, et al. Novel microglia-mediated mechanisms underlying synaptic loss and cognitive impairment after traumatic brain injury. Brain Behav Immun. 2021;98:122–35.
11. Nespoli E, Hakani M, Hein TM, May SN, Danzer K, Wirth T, et al. Glial cells react to closed head injury in a distinct and spatiotemporally orchestrated manner. Sci Rep. 2024;14:2441.
12. Kim H, Kim MJ, Kwon YW, Jeon S, Lee SY, Kim CS, et al. Benefits of a skull-interfaced flexible and implantable multilight emitting diode array for photobiomodulation in ischemic stroke. Adv Sci. 2022;9:e2104629.

13. Yang L, Wu C, Tucker L, Dong Y, Li Y, Xu P, et al. Photobiomodulation therapy attenuates anxious-depressive-like behavior in the TgF344 rat model. J Alzheimers Dis. 2021;83:1415–29.
14. Yang L, Dong Y, Wu C, Li Y, Guo Y, Yang B, et al. Photobiomodulation preconditioning prevents cognitive impairment in a neonatal rat model of hypoxia-ischemia. J Biophoton. 2019;12:e201800359.
15. Yang L, Tucker D, Dong Y, Wu C, Lu Y, Li Y, et al. Photobiomodulation therapy promotes neurogenesis by improving post-stroke local microenvironment and stimulating neuroprogenitor cells. Exp Neurol. 2018;299:86–96.
16. Gordon LC, Johnstone DM. Remote photobiomodulation: an emerging strategy for neuroprotection. Neural Regen Res. 2019;14:2086–7.
17. Hosang L, Canals RC, van der Flier FJ, Hollensteiner J, Daniel R, Flugel A, et al. The lung microbiome regulates brain autoimmunity. Nature. 2022;603:138–44.
18. Mumaw CL, Levesque S, McGraw C, Robertson S, Lucas S, Stafflinger JE, et al. Microglial priming through the lung-brain axis: the role of air pollution-induced circulating factors. FASEB J. 2016;30:1880–91.
19. Yang L, Wu C, Parker E, Li Y, Dong Y, Tucker L, et al. Non-invasive photobiomodulation treatment in an Alzheimer disease-like transgenic rat model. Theranostics. 2022;12:2205–31.
20. Yang L, Dong Y, Wu C, Youngblood H, Li Y, Zong X, et al. Effects of prenatal photobiomodulation treatment on neonatal hypoxic ischemia in rat offspring. Theranostics. 2021;11:1269–94.
21. Zong X, Dong Y, Li Y, Yang L, Li Y, Yang B, et al. Beneficial effects of theta-burst transcranial magnetic stimulation on stroke injury via improving neuronal microenvironment and mitochondrial integrity. Transl Stroke Res. 2020;11:450–67.
22. Yang L, Wu C, Li Y, Dong Y, Wu CY, Lee RH, et al. Long-term exercise pre-training attenuates Alzheimer's disease-related pathology in a transgenic rat model of Alzheimer's disease. Geroscience. 2022;44:1457–77.
23. Wu C, Yang L, Li Y, Dong Y, Yang B, Tucker LD, et al. Effects of exercise training on anxious-depressive-like behavior in Alzheimer rat. Med Sci Sports Exerc. 2020;52:1456–69.
24. Zhou R, Wang Z, Zhou B, Yu Z, Wu C, Hou J, et al. Estrogen receptors mediate the antidepressant effects of aerobic exercise: a possible new mechanism. Front Aging Neurosci. 2022;14:1040828.
25. Feng S, Wu C, Zou P, Deng Q, Chen Z, Li M, et al. High-intensity interval training ameliorates Alzheimer's disease-like pathology by regulating astrocyte phenotype-associated AQP4 polarization. Theranostics. 2023;13:3434–50.
26. Wu C, Yang L, Tucker D, Dong Y, Zhu L, Duan R, et al. Beneficial effects of exercise pretreatment in a sporadic Alzheimer's rat model. Med Sci Sports Exerc. 2018;50:945–56.
27. Wu C, Deng Q, Zhu L, Liu TC, Duan R, Yang L. Methylene blue pretreatment protects against repeated neonatal isoflurane exposure-induced brain injury and memory loss. Mol Neurobiol. 2024;61:5787–801.
28. Chiu KB, Lee KM, Robillard KN, MacLean AG. A method to investigate astrocyte and microglial morphological changes in the aging brain of the rhesus macaque. Methods Mol Biol. 2019;1938:265–76.
29. Li L, Lu S, Zhu J, Yu X, Hou S, Huang Y, et al. Astrocytes excessively engulf synapses in a mouse model of Alzheimer's disease. Int J Mol Sci. 2024;25:1160.
30. Wu C, Yang L, Youngblood H, Liu TC, Duan R. Microglial SIRPalpha deletion facilitates synapse loss in preclinical models of neurodegeneration. Neurosci Bull. 2022;38:232–4.
31. Wang J, Huang Q, Chen X, You Z, He K, Guo Q, et al. Tau pathology is associated with synaptic density and longitudinal synaptic loss in Alzheimer's disease. Mol Psychiatry. 2024;29:2799–2809.
32. Baugh CM, Stamm JM, Riley DO, Gavett BE, Shenton ME, Lin A, et al. Chronic traumatic encephalopathy: neurodegeneration following repetitive concussive and subconcussive brain trauma. Brain Imaging Behav. 2012;6:244–54.
33. Pasam T, Dandekar MP. Insights from rodent models for improving bench-to-bedside translation in traumatic brain injury. Methods Mol Biol. 2024;2761:599–622.
34. Ledreux A, Pryhoda MK, Gorgens K, Shelburne K, Gilmore A, Linseman DA, et al. Assessment of long-term effects of sports-related concussions: biological mechanisms and exosomal biomarkers. Front Neurosci. 2020;14:761.
35. McKeithan L, Hibshman N, Yengo-Kahn AM, Solomon GS, Zuckerman SL. Sport-related concussion: evaluation, treatment, and future directions. Med Sci. 2019;7:44.
36. Naeser MA, Martin PI, Ho MD, Krengel MH, Bogdanova Y, Knight JA, et al. Transcranial photobiomodulation treatment: significant improvements in four ex-football players with possible chronic traumatic encephalopathy. J Alzheimers Dis Rep. 2023;7:77–105.
37. Wu C, Yang L, Feng S, Zhu L, Yang L, Liu TC, et al. Therapeutic non-invasive brain treatments in Alzheimer's disease: recent advances and challenges. Inflamm Regen. 2022;42:31.
38. Bolton Hall AN, Joseph B, Brelsfoard JM, Saatman KE. Repeated closed head injury in mice results in sustained motor and memory deficits and chronic cellular changes. PLoS ONE. 2016;11:e0159442.
39. Yang L, Feng S, Wu C, Yang L. The lung microbiome: a potential target in regulating autoimmune inflammation of the brain. Neurosci Bull. 2022;38:1435–7.
40. Liddelow SA, Guttenplan KA, Clarke LE, Bennett FC, Bohlen CJ, Schirmer L, et al. Neurotoxic reactive astrocytes are induced by activated microglia. Nature. 2017;541:481–7.
41. Chang SY, Lee MY. Photobiomodulation of neurogenesis through the enhancement of stem cell and neural progenitor differentiation in the central and peripheral nervous systems. Int J Mol Sci. 2023;24:15427.
42. Tu J, Huang Y, Huang Y, Wu M, Wang R. [Photobiomodulation promotes hippocampal neurogenesis and improves cognitive function and anti-inflammatory injury in rats with chronic cerebral hypoperfusion]. Sichuan Da Xue Xue Bao Yi Xue Ban. 2023;54:965–71.
43. Chen W, Zhang Y, Zhai X, Xie L, Guo Y, Chen C, et al. Microglial phagocytosis and regulatory mechanisms after stroke. J Cereb Blood Flow Metab. 2022;42:1579–96.
44. Wu C, Zhang S, Sun H, Li A, Hou F, Qi L, et al. STING inhibition suppresses microglia-mediated synapses engulfment and alleviates motor functional deficits after stroke. J Neuroinflammation. 2024;21:86.
45. Xuan W, Agrawal T, Huang L, Gupta GK, Hamblin MR. Low-level laser therapy for traumatic brain injury in mice increases brain derived neurotrophic factor (BDNF) and synaptogenesis. J Biophoton. 2015;8:502–11.
46. Xuan W, Vatansever F, Huang L, Wu Q, Xuan Y, Dai T, et al. Transcranial low-level laser therapy improves neurological performance in traumatic brain injury in mice: effect of treatment repetition regimen. PLoS ONE. 2013;8:e53454.
47. Chung WS, Clarke LE, Wang GX, Stafford BK, Sher A, Chakraborty C, et al. Astrocytes mediate synapse elimination through MEGF10 and MERTK pathways. Nature. 2013;504:394–400.
48. Wang J, Ding X, Wu X, Liu J, Zhou R, Wei P, et al. SIRPalpha deficiency accelerates the pathologic process in models of Parkinson disease. Glia. 2019;67:2343–59.
49. Jia J, Yang L, Chen Y, Zheng L, Chen Y, Xu Y, et al. The role of microglial phagocytosis in ischemic stroke. Front Immunol. 2021;12:790201.
50. Henderson TA. Can infrared light really be doing what we claim it is doing? infrared light penetration principles, practices, and limitations. Front Neurol. 2024;15:1398894.
51. Costanti Vilela Campos M, Simoes Velloso Schuler S, de Barros Motta P, Catia Mazzoni A, Cristina da Silva F, Domingues Martins M, et al. The effect of systemic versus local transcutaneous laser therapy on tension-type cephalea and orofacial pain in post-COVID-19 patients: a pragmatic randomized clinical trial. Medicine. 2022;101:e31218.
52. Araujo T, Andreo L, Tobelem DDC, Silva T, Malavazzi T, Martinelli A, et al. Effects of systemic vascular photobiomodulation using LED or laser on sensory-motor recovery following a peripheral nerve injury in Wistar rats. Photochem Photobiol Sci. 2023;22:567–77.
53. Johnstone DM, el Massri N, Moro C, Spana S, Wang XS, Torres N, et al. Indirect application of near infrared light induces neuroprotection in a mouse model of parkinsonism - an abscopal neuroprotective effect. Neuroscience. 2014;274:93–101.
54. Rodrigo SM, Cunha A, Pozza DH, Blaya DS, Moraes JF, Weber JB, et al. Analysis of the systemic effect of red and infrared laser therapy on wound repair. Photomed Laser Surg. 2009;27:929–35.
55. Rochkind S, Rousso M, Nissan M, Villarreal M, Barr-Nea L, Rees DG. Systemic effects of low-power laser irradiation on the peripheral and central nervous system, cutaneous wounds, and burns. Lasers Surg Med. 1989;9:174–82.
56. Jimenez JJ, Wikramanayake TC, Bergfeld W, Hordinsky M, Hickman JG, Hamblin MR, et al. Efficacy and safety of a low-level laser device in the treatment of male and female pattern hair loss: a multicenter, randomized, sham device-controlled, double-blind study. Am J Clin Dermatol. 2014;15:115–27.

ACKNOWLEDGEMENTS

This study was supported by the National Natural Science Foundation of China (32100918 and 32300959), the Guangzhou Scientific Research Grant (SL2022B04J00013 and SL2024A04J00578), and the SCNU Young Faculty Development Program (22KJ04).

AUTHOR CONTRIBUTIONS

LY designed the study. CW and ML established the animal model. CW, ML, and ZC conducted animal behavioral tests. CW, ML, and QD analyzed the data. CW and SF performed the immunofluorescence staining. ML, ZC, and SF collected brain tissues and lung microbiome samples. CW drafted the manuscript. RD, TCL, and LY revised the manuscript. LY supervised the project. All authors read and approved the final manuscript.

COMPETING INTERESTS

The authors declare no competing interests.

ADDITIONAL INFORMATION

Supplementary information The online version contains supplementary material available at https://doi.org/10.1038/s41398-025-03228-3.

Correspondence and requests for materials should be addressed to Luodan Yang.

Reprints and permission information is available at http://www.nature.com/reprints

Publisher's note Springer Nature remains neutral with regard to jurisdictional claims in published maps and institutional affiliations.